Layout design for a venturi to encase a wind turbine integrated in a high rise

Beller, Christina

Published in:
Conference proceedings (online)

Publication date:
2008

Layout Design for a Venturi to encase a Wind Turbine integrated in a High Rise

C. Beller

Risø National Laboratory for Sustainable Energy
Technical University of Denmark
DK-4000 Roskilde, Denmark
christina.beller@risoe.dk

Stiftungslehrstuhl Windenergie
University of Stuttgart
D-70550 Stuttgart- Vaihingen, Germany
swe@ifb.uni-stuttgart.de

Abstract:

In this work a general CFD supported investigation of the potential of Venturi shaped turbine casings, compared to a constant in diameter tubing, is carried out. Inspired by and based on the skyscraper design 'Castle House', including turbines integrated into the buildings structure, a parameter study about encased turbines in urban areas is developed. The simulation approach is validated by modelling a DIN EN ISO 5167-3:2003 Venturi device in the CFD environment of FIDAP. Starting with this standardized Venturi geometry, combined with characteristic wind tunnel design rules, three tubing geometry are constructed. The top floor of the building is simplified as a 'coin' model with a hole in the middle, wherein the turbine is placed later on. This is to simplify the model to be axis- symmetric. Contractions of 1.00, 2.25, 4.00, and 9.00 are simulated. Analyses of the flow through the single contractions are carried out and by comparison the most effective geometry is chosen to work on further with. In the next step, a turbine, represented by an actuator disc, is implemented by body forces. A focus is taken on positioning the turbine with varying thrust coefficients at three different characteristic Venturi depths. The resulting flow behaviour is qualitative described and a discussion follows.
Key words: encased, Venturi, urban wind energy

1 Introduction

Urban landscape changes due to new architectures. Buildings are built much higher, therefore roofs are reaching in high wind speed layers, planned urban structure is applied, which can be used to direct mainstreams, and consciousness about environmental friendly systems is more and more present, which increases the tolerance and even stimulates desire of private renewable energy. Few ideas of urban turbines, encased [1], with vertical axis [2] and moreover unconventional concepts [3], [4] are realized. Some designs are of the category 'house hold turbines' and are meant to supply the house, with no respect to the integration of the wind turbine into the flow situation around the building itself [5]. Some others are already considering the upwind on a house façade and are placed on logical places aligned to the main wind direction [6], [7]. All of them were so far fixed on an already existing building. The potential of considering a turbine already in the conceptual house design pays of in saving the structure for a turbine tower, in increased wind velocity and directing by smart blockage of the building and with this a higher power harvesting. Especially, the so long controversial encased turbine contra arguments can be cancelled out- no additional heavy structure is necessary, because it can be integrated in the architecture. It is definitely a process of compromises, on the side of the architectural freedom and the side of the technical efficiency.

A new project, 'Castle House', is planned for the year 2009. The high riser shall be erected in London, surrounded by low buildings (fig. 1). The new way of turbines integration in buildings structure by encasing them offers some interesting new parameters in terms of noise reduction, concentrating and directing the wind,

Figure 1: 'Castle House', conceptual design [8]

tip loss reduction and more, which need to be well investigated. The conceptual design shows straight ducts for the turbine encasings and smooth transitions from the facade to the inlet were not taken into consideration. The idea is to prevent or at least diminish separation at the inlet and accelerate the air by application of a Venturi shaped tube. With the mass conservation law,

$$\frac{dm}{dt}_i = \rho A_i v_i = const., \tag{1}$$

two cross sections in a tube are related in the following way,

$$v_2 = v_1 \frac{A_1}{A_2}, \tag{2}$$

while the inlet cross section over throat section ratio states the contraction,

$$Co = \frac{A_{inlet}}{A_{throat}}. \tag{3}$$

Thus, the higher the contraction, the higher is the velocity amplification and therefore the power amplification. Available power defined as,

$$P_i = \frac{1}{2}\frac{dm}{dt}_i v_i^2 = \frac{1}{2}\rho A_i v_i^3, \tag{4}$$

leads with (1) to the power ratio,

$$\frac{P_2}{P_1} = \frac{\frac{1}{2}\frac{dm}{dt}_2 v_2^2}{\frac{1}{2}\frac{dm}{dt}_1 v_1^2} = \frac{A_2 v_2^3}{A_1 v_1^3}, \tag{5}$$

and therefore to

$$\frac{P_2}{P_1} = Co^2. \tag{6}$$

How this statement proves true or not is shown in section 3. To keep the simulation simple and develop a basic study but orientated on a current project, the problem is rotationally symmetric defined. With the assumption of an axis-symmetrical problem the house is reduced to its upper part and then represented by a coin shaped model (fig. 2). The outer radius is one of the constant parameters for the four investigated contractions. For the inlet and outlet diameter a constant value of $9m$ is settled. Another fixed parameter is the length, which is determined by the Venturi design laws explained in section 2. The mean wind velocity, v_w, is stated with $6.00m/s$. Starting up from this basis, three inlay shapes with the contractions 2.25, 4.00 and 9.00 are found, inserted into the coin model, Co1.00, to be examined and compared. Next to the interest which contracting curvature for the inlay is most advantegous in respect to power amplification lies the interest how the turbine positioning influences the flow behaviour. Fig. 3 shows such an inlay, here for the contraction 2.25. It consists

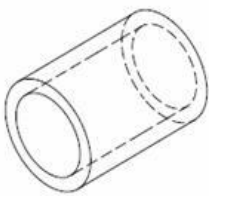

Figure 2: Coin model, Co = 1

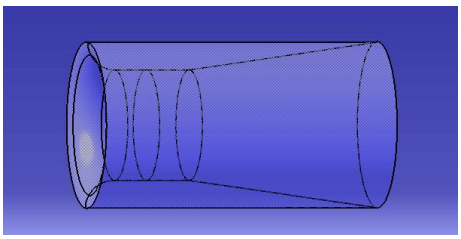

Figure 3: Coin model inlay, Co = 2.25

of the contracting, smooth shaped inlet, the constant diameter section called the throat and the diffuser expanding from the throat diameter back to the inlet diameter. Due to the Venturi effect the highest velocity occurs in the section with the smallest diameter and therefore in the throat. Gerald J. W. Van Bussel [9] did in his one dimensional analysis not consider the turbine location. Within this simulation viscous effects are considered and the velocity profile inside the tube is consequently depending on radial and axial coordinates. Three distinctive positions along the axis are chosen to find the most attractive variant in terms of the interaction of the blockage effect of the contracted duct itself and the blockage of the turbine. Position one, $pos1$, is chosen at the interface of the inlet and throat. Because losses due to viscous effects are not negligible, the highest amount of energy can be found at this position and the relatively long throat following gives the flow the opportunity to develop to a more uniform profile and therefore reduces the risk of separation in the diffuser. Separation in the diffuser causes significant pressure losses. The second position, $pos2$, is defined in the throat, where a developed velocity profile exists. Because the critical Reynolds number is far exceeded, the velocity profile is a blunt turbulent one with mainly axial velocity components. With an almost constant core velocity, the flow approach towards the turbine is comparable to the situation for a bare turbine in a free

field and in consideration of a suggested conventional turbine desirable. To attend the theoretical streamline tube (fig. 4) of a bare turbine, position three, $pos3$, was found. By decelerating the

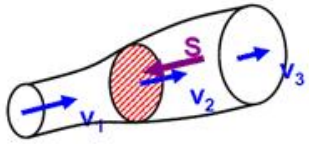

Figure 4: Ideal streamline tube, unducted turbine [10]

flow the streamline tube enlarges in diameter. Of course, the situation for an encased turbine is different by all means, but the velocity is decelerated by the turbine as well and the diffuser allows or supports, respectively, the expansion and so contributes a smooth flow through the device. Another idea, but not accomplished within this work, is the positioning in half the depth of the diffuser, to include the whole stream tube shown in fig. 4 and use the inlet and throat as kind of wind accelerator, supporting the stream tube system. The contra argument is the bigger diameter and the therewith linked higher financial costs.

2 Venturi Layout

With the help of the Venturi standard [11] the parameter settings within FIDAP are validated. It hazards the guess, that the geometry given in the standard for a Venturi is most investigated and developed over the years to be optimized in matters of losses due to friction but also separation. To use the standard geometry would be recommendable, as long as it is meant to accelerate a fluid. But as soon as an obstacle is implemented in the throat, the application is changed and the standard geometry does not constitute an optimum anymore. The configuration of an Eiffel wind tunnel with closed model section is redolent of a Venturi tube but with an obstacle in the throat. Instead of the natural wind, a fan is generating the air flow through the tunnel. Wind tunnel tests demand also low turbulence intensity in the flow and losses might be reduced. Therefore based on wind tunnel designs [12] certain laws for the Venturi geometry meant to encase a turbine are derived, as

§1 high curvature should take place in big diameter

§2 a constant area duct before the rotor section should be employed

§3 the throat length behind the rotor should be sufficient long

§4 diffusers opening angle has to be sufficient small

and are discussed following. It turns out that the ISO standard fulfils the conditions. With respect to minimize losses due to friction, implicit minimizing the all over length, the nozzle, throat and diffuser length should be kept short as possible, but without incurring flow separation. Due to the law of continuity for an incompressible fluid, the loss will not be reflected in the dynamic pressure, but in the static pressure, while the loss coefficient is defined on the basis of total pressure and dynamic pressure. Hence power losses are proportional to power two of the velocity in the cross section. This conclusion leads to the first design law, concerning the inlet.

inlet: Curvatures of the structure and therefore deflections of the flow are linked to losses, while the losses are proportional to the squared velocity.

§1 high curvature should take place in big diameter

The smaller radius is placed at the inlet mouth and is passing over tangential to the bigger radius arc, meaning a high curvature by the small radius, hence in the section with lower velocities and a lower curvature in the section, leading to the maximum velocity (fig. 5).

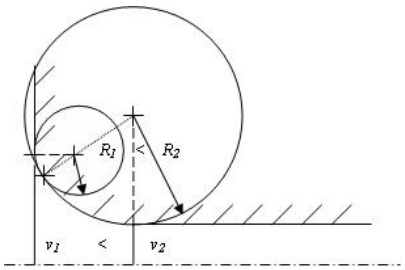

Figure 5: Inlet nozzle consisting of two tangential merged circles

throat: It is in general desirable to reduce the length of the whole Venturi device, thus an idea is to skip the whole throat section and join the nozzle directly to the diffuser (fig. 6). Also, the power losses in the throat are sizable. Power could be saved by keeping it short. But design law number two and three tell us: Contractions do not deliver a uniform velocity distribution to the beginning of the throat, so

§2 a constant area duct before the rotor section should be employed

Behind the rotor the flow might be separated and all separated flow zones shall be close before the beginning of the diffuser, therefore

§3 the throat length behind the rotor should be sufficient long

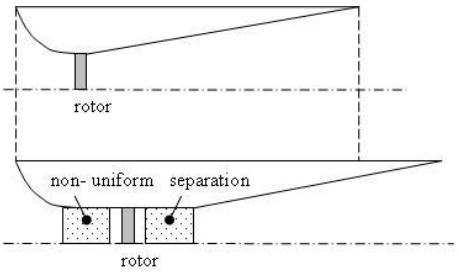

Figure 6: Straight section in front and behind the rotor

diffuser: Since the power losses at any point in the tunnel are expected to vary as the speed cubed, the purpose of the diffuser is to reduce the speed with as little energy loss as possible. Minimum energy loss corresponds to maximum pressure recovery. It is in general desirable to reduce the speed in the shortest possible distance without incurring flow separation.

§4 diffusers opening angle has to be sufficient small

Because of the throat segment behind the rotor plane, the separated flow zones are expected to be closed again. Therefore a bigger opening angle is applicable. Here the diffuser opening angle is limited to max. $\varphi = 30°$. With the lenght as a constant parameter the model geometries are determined and listed in tab. 1.

Co	1.00	2.25	4.00	9.00
$d[m]$	9.00	6.00	4.50	3.00
$L_{inlet}[m]$	–	1.57	2.32	3.07
$L_{throat}[m]$	–	4.20	3.15	2.10
$L_{diffuser}[m]$	–	10.28	10.87	11.20
$\frac{\varphi}{2}[°]$	0.00	8.21	12.04	15.00

Table 1: d: throat diameter; L_{inlet}: inlet length; L_{throat}: throat length; $L_{diffuser}$: diffuser length; $\frac{\varphi}{2}$: half diffuser opening angle

3 Model without Turbine

In this chapter the turbine is not implemented yet to find out about the blocking and separation behaviour of the single contractions structures themselves and to choose later the most reasonable models to insert turbines at different positions. The computational domain is set up as seen in fig. 7, while the parameter settings are chosen in the following way:

PROBLEM: nonlinear, turbulent, axis-symmetric; VISCOSITY MODEL: Boussinesq-RNG (two equation); SOLUTION: segregated solver, upwinding; ACCURACY: $velc = 1 * 10^{-5}$; $resc = 1 * 10^{-5}$; FLUID: $\rho = 1.225 kg/m^3$; $\mu = 1.8375 * 10^{-5} Ns/m^2$; INITIAL CONDITIONS: $k = 0.003$; $\epsilon = 0.00045$; INLET: $radial\ velocity = 0m/s$; $axial\ velocity = 6m/s$; $k = 0.003$; $\epsilon = 0.00045$; SYMMETRY AXIS: $radial\ velocity = 0m/s$; STRUCTURE: $wall\ velocity = 0m/s$.

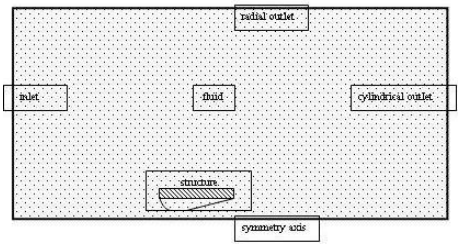

Figure 7: Computational domain set up, bare structure

With this settings interesting observations are made, startig with the contraction $Co = 1.00$.

Co1.00: The streamline plot (fig. 8) shows a separation bubble inside the device, which forms the so called 'Vena Contracta' and therefore works like a Venturi constriction. In the inlet is

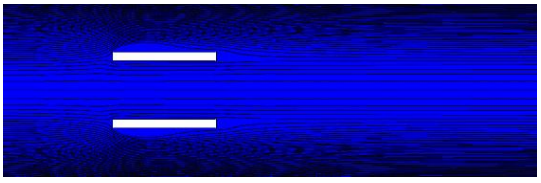

Figure 8: Streamline plot; $Co = 1.00$, bare

a mean velocity of $5.35m/s$ calculated. Wind tunnel measurements carried out within the 'Castle House' feasibility study carried out by

the group of consultancy including Norwin A/S found an increase of the undisturbed wind velocity taking place through the tubing, while the house model was additionally blocking the wind. The strong upwind, generated at the house facade concentrated the wind towards the upper part and therefore the building blockage forced more flow going through the holes. This parameter study here decouples the effect of the building and therefore the skewed inflow velocity components and concentrates on the inlay shaping only.

Co2.25: In comparison to the tube without contraction, no separation takes place in the inlet for the contraction 2.25 (fig. 9). Especially the

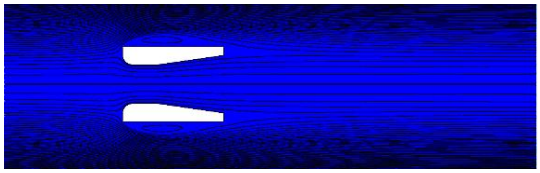

Figure 9: Streamline plot; $Co = 2.25$, bare

diffuser in a Venturi shape turns out to be the most critical part, but also here the flow keeps attached. Remarkable is the all over shape of the structure added up with the separation bubbles. It is redolent of a common profile shape. Fig. 10 shows the axial velocities around the structure $Co2.25$. The field of interest is the throat section where the highest velocities occur. At the throat inlet and outlet close to the wall the flow is deflected most and therefore must be accelerated most as well, resulting in suction and velocity peaks, respectively. The axial velocity

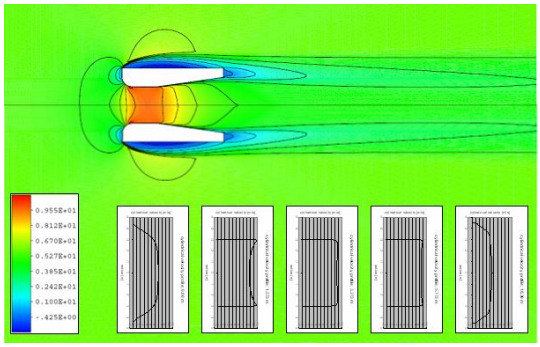

Figure 10: Velocity plot; $Co = 2.25$, bare

profiles are plotted at the important positions along the device axis; device inlet at $0m$, throat inlet at $1.6m$, position where the velocity profile is expected to be developed, $3.4m$, throat outlet at $5.8m$ and the device outlet at $16.3m$. Usually a turbine blade is exposed to a regular wind velocity profile. By rotation the blade experiences a combined velocity. The more far out, towards the tip, the smaller gets the angle of attack. To gain the best lift over drag ratio geometrical twist is applied. An argument to position a turbine in the cross sections with these distinctive peaks, throat inlet and throat outlet, is that the blade twist could be reduced. Additionally would the resulting velocity at the tip be very high and with this a high lift force could be obtained at a position generating moment most effective. For the inlet and the outlet mean velocity a value of $4.23m/s$ is calculated. Through the throat a mean velocity of $9.52m/s$ is determined, while the velocity profiles differs from each other in significant way. Fig. 11 shows the high pressure area around the stagnation point and its spacious influence. It is

Figure 11: Static pressure plot; $Co = 2.25$, bare

important to consider, that the streamline through the stagnation point is representing the border between streamlines entering the structure and streamlines surrounding the structure. The influence of the stagnation point position is obvious, but no analytical relationship is derived within this work.

Co4.00: On the outer surface of the device the separation bubble has grown compared to the contraction 2.25, but it still reattaches to the rear (fig. 12). In contrast to the flow through the

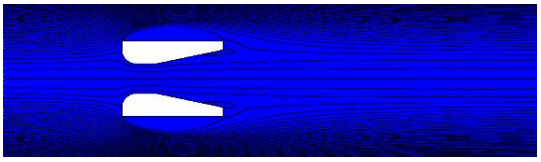

Figure 12: Streamline plot; $Co = 4.00$, bare

diffuser in $Co2.25$, flow separation is detected in this case, which leads to higher pressure losses through the diffuser but also to reduced efficiency of the whole device. The stagnation point of the contraction of 4.00 is positioned already on the curvature of the inlet ($xst_{Co4.00} = 0.019m$; $yst_{Co4.00} = 4.187m$), which reflects the blocking effect of the higher contraction. Negative axial ve-

locity components exist in the very entrance of the device, resulting in a smaller 'effective' inlet and thus contraction (fig. 13). The mean velocity in

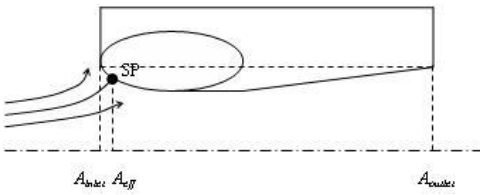

Figure 13: Streamline through stagnation point

the inlet is with $2.67m/s$ far below the undisturbed wind velocity. Such a strong contraction of the flow increases the drag intensely. Directly linked to that is a reduced mass flow through the device. The high pressure region around the stagnation point is shutting down the inlet.

Co9.00: For the contraction 9.00 the streamline plot shows big separation areas (fig. 14). The

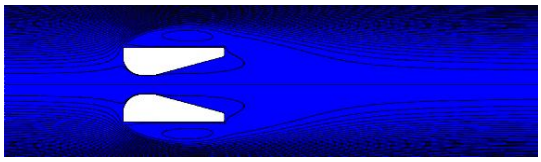

Figure 14: Streamline plot; $Co = 9.00$, bare

bubble on the outer surface has grown over the rear edge and mingles with the outflow of the device. Inside the diffuser the flow is almost not attached at all. The stagnation point lies with $xst_{Co9.00} = 0.19$ m; $yst_{Co9.00} = 3.45$ m deep in the nozzle and hazards the guess that the high amplification failed. Indeed, the throat velocity lies with $8.95m/s$ even below the contraction 4.00 throat velocity. The low velocity area behind the structure is deflected towards the axis and generates therein a kind of shielding. Already for contraction 4.00 this deflecting trend can be observed. At the same time the pressure shield at the front face is getting more rigorous (fig. 15).

Figure 15: Static pressure plot; $Co = 9.00$, bare

Comparison: Two properties are influencing the structures in their quality to increase the potential energy in the throat. One aspect to look at is the blockage by the contraction. Another one is the velocity amplification. With increasing contraction the velocity amplification increases, but the resistance increases as well, so that mass flows arround the structure instead of flowing through it to get accelerated. The optimum between mass reduction and mass acceleration has to be found. The blockage is defined by the velocity in the throat, which would be achieved with an inlet velocity equal to the wind velocity, over the actual lower throat velocity, due to mass surrounding the structure.

$$blockage = \frac{v_{throat_{tubed}}}{v_{throat_{CFD}}} \tag{7}$$

The velocity amplification is defined by the actual throat velocity over the undisturbed wind velocity.

$$velocity\ amplification = \frac{v_{throat_{CFD}}}{v_w} \tag{8}$$

In terms of taking into account the two aspects mentioned above, a contraction of approximately 2.25 constitutes the maximum in effectiveness, where velocity amplification over blockage ratio is biggest. A contraction of one is then more effective than a contraction of four. A closer look on the energy flux shows something different. Air flowing through a cross section in the size of the inlet, with the velocity of the undisturbed wind has an energy flux potential of

$$\frac{dE_w}{dt} = \frac{1}{2}\frac{dm}{dt}v_w^2 = \frac{1}{2}\rho A_{inlet}v_w^3. \tag{9}$$

The actual energy fluxes in the single throat sections are calculated corresponding and listed in table 2. To keep the application of the geometries feasible, focus is taken on the contraction 2.25. With a throat diameter of six meters this structure offers space for a small turbine. Besides this more practical aspect the fact of the highest energy amplification and no separation through the whole $Co2.25$ device makes it most attractive. By inserting a turbine, the blockage will be increased even more and therefore the mass flow through the throat reduced. In the following chapter this circumstance is examined for the contraction 2.25, while the turbine is positioned at three different significant throat depths.

4 Model with turbine

With the help of body forces implementation a turbine modelled as an actuator disc can be simu-

		$definition$	$Co1.00$	$Co2.25$	$Co4.00$	$C09.00$
$v_{throat_{CFD}}$	$[m/s]$	$-$	5.35	9.52	**10.67**	8.95
$v_{inlet_{CFD}}$	$[m/s]$	$-$	5.35	4.23	2.67	1.00
$v_{throat_{tubed}}$	$[m/s]$	$\frac{A_{inlet}}{A_{throat}} v_w$	6.00	13.50	24.00	54.00
$\frac{dm}{dt}\ CFD$	$[kg/s]$	$A_{throat} \rho v_{throat}$	**416.95**	329.68	207.82	77.51
$blockage$	$[-]$	(7)	**1.12**	1.42	2.25	6.03
$velocity\ amplification$	$[-]$	(8)	0.89	1.59	**1.78**	1.49
$energy flux\ amplification$	$[-]$	$\frac{dE/dt_{throat_{CFD}}}{dE/dt_w}$	0.71	**1.77**	1.41	0.37

Table 2: Flow characteristics overview, models without turbine

lated. The constant distributed body forces constitute the thrust. For the free standing turbine, the thrust coefficient is defined [13] as

$$C_T = \frac{T}{\frac{1}{2}\rho v_w^2 A_{rotor}}, \tag{10}$$

referring to the undisturbed wind velocity flowing through an area in the size of the rotor, while T is the turbines thrust. The power coefficient is the ratio of harvested power over available power in a cross section equal to the area swept by the rotor and can also be written as

$$C_P = \frac{T v_{AD}}{\frac{1}{2}\rho v_w^3 A_{rotor}}, \tag{11}$$

with v_{AD} as the retarded wind velocity in the rotor plane. Inserting (10) in (11) the power coefficient can be defined as

$$C_P = C_T \frac{v_{AD}}{v_w}, \tag{12}$$

while

$$T = \Delta p A_{rotor}. \tag{13}$$

Assuming the ideal conditions from Froude- Rankine theorem a Betz maximum $C_{P_f} = \frac{16}{27}$ and a $C_{T_f} = \frac{8}{9}$ are expected for a bare turbine. Prerequisite of an ideal power harvesting is an axial induction factor of one third, which shall be reflected in a velocity in the actuator disc of two third of the undisturbed wind velocity, hence $v_AD = 4m/s$. Fig. 16 shows the resulting values for the pressure and the velocity along the symmetry axis. As soon as the rotor is encased it must be clarified to which area the dimensionless coefficients refer to. For the first consideration the coefficients, C_P and C_T, shall refer to the actual rotor sweeping area.This is the conventional way of looking at it, but makes a comparison difficult. Mostly, in investigations done before, the increased mass flow through the turbine caused by a diffuser or shroud was referred to the rotor cross section and compared to a bare rotor of the same size. Here is the inlet area kept constant and given is the same

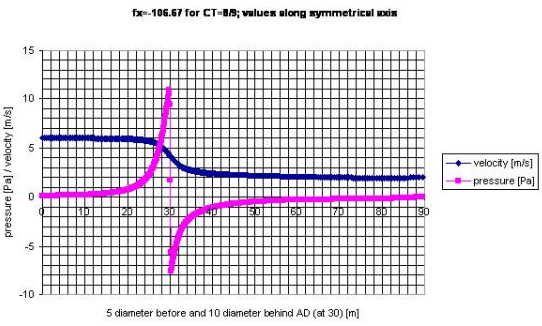

Figure 16: Velocity and static pressure plot along symmetrical axis, AD in free field, Betz optimum

initial situation, but the rotor diameter varies corresponding to the contractions. Which inner geometry combined with a turbine makes most out of the offered wind entering the same inlet is ascertained. In general the power coefficient is the ratio of harvested power over power contained in the wind. That is why in a second definition the power coefficient refers to the inlet area, C_p^*.

$$C_P^* = \frac{\Delta p v_{AD} A_{rotor}}{\frac{1}{2}\rho v_w^3 A_{inlet}} = \frac{C_P}{Co}, \tag{14}$$

Values for the thrust coefficient referring to the rotor area are $C_{T_0} = 0.24$, $C_{T_1} = 0.30$, $C_{T_2} = 0.0.36$, $C_{T_3} = 0.44$, $C_{T_4} = 0.53$, $C_{T_5} = 0.59$, $C_{T_6} = 0.62$, $C_{T_7} = 0.64$, $C_{T_8} = 0.65$, $C_{T_9} = 0.69$.The settings considering the geometry, turbulence modeling, wind properties and boundary conditions are not changed compared to the bare structure simulations. But the settings here are added up with an actuator disc. The systems, casing and turbine, are named in the following way $Co2.25pos1$, $Co2.25pos2$, $Co2.25pos3$ and $Co1.00pos1$, $Co1.00pos2$, $Co1.00pos3$, respectively. In case of the contraction 1.00 is $pos1$ positioned directly at the device inlet, $pos2$ at a location where the velocity profile is expected to be developed without the influence of the applied

thrust and $pos3$ directly at the outlet of the device. $Pos1$ is located directly at the throat inlet for the contraction 2.25, while $pos2$ is located in the throat where the velocity profile is expected to be developed in case of a bare structure and $pos3$ is positioned at the outlet of the throat, before the diffuser starts.A detailed examination of the simulation results for $Co2.25AD$ ($Co = 2.25$; actuator disk implemented) is performed, while case $Co1.00AD$ ($Co = 1.00$; actuator disk implemented) is run only until a thrust coefficient of $C_T = 0.53$.

Co2.25AD: The results for C_P at $pos1$, $pos2$ and $pos3$ are plotted over the applied C_T in fig. 17. For the lower pressure sinks due to the actuator disk the behaviour of the flow does not differ distinctively. At $C_{T_3} = 0.44$ the first characteristic branching occurs. The turbine at $pos1$ is blocking the flow less than the turbines placed at $pos2$ and $pos3$, although the same thrust is affecting the flow. The static pressure sink due to the turbine has the typical pressure maximum in front of the AD and the minimum behind approaching asymptotic the atmospheric pressure again. To recall this pressure development, please see fig. 16. This pressure maximum upstream the turbine is reaching more out of the structure inlet in case one, than in two or three. So the pressure peak has more space compared to the pressure peaks in front of the turbines positioned at $pos2$ or $pos3$. Because of the more restricted space for the pressure peak the 'pressure density' is increasing and therefore the blockage is increasing as well. This circumstance is reflected by the decreasing inlet velocity and with it the smaller mass flow through the structure (fig. 18). In this figure it can also be seen, that the static pressure maximum along the axis for the AD at $pos1$ is located $3.14m$, for the AD at $pos2$ $2.42m$ and for the AD at $pos3$ $1.97m$ in front of the structure inlet. By implementing

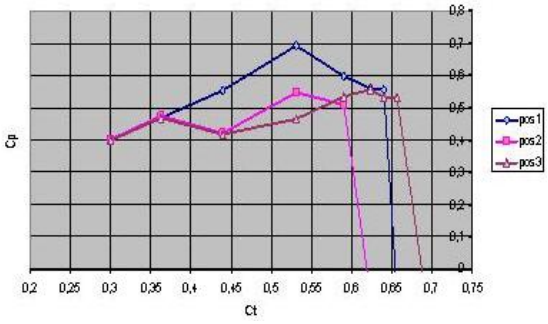

Figure 17: C_P over C_T plot, $Co2.25AD$, $pos1$, $pos2$, $pos3$

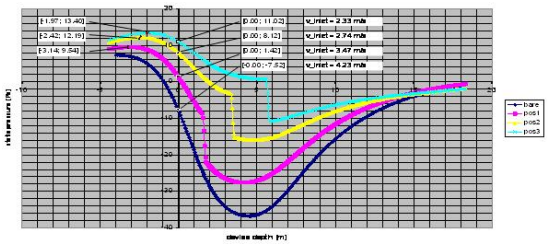

Figure 18: Static pressure plotted along the axis; structure inlet at $0m$; $Co2.25AD$, $C_T = 0.53$

$C_{T_5} = 0.59$ a new effect starts to take over. Since the velocity is decelerated by the turbine, but in contrast to the pressure change in a continuous manner, the lowest speed for the turbine wake at position two is closer situated to the diffuser end, than for the turbine at position three. What happens is that the turbine wake with very low velocities grows and marches upstream until it acts at the diffuser outlet like a blocking area. In the mixing area of the two flow streams behind the structure, the outer stream is deflected towards the axis due to the 'over expanded' jet situation there. At this point, additionally, the wake of the structure with its separation bubble on the outer surface and the rear face starts to interact. The outflow has to find its way between the turbine wake and the structure wake (fig. 19). A barrier

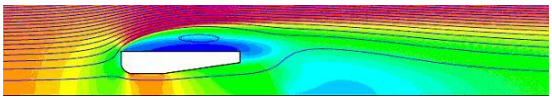

Figure 19: Superposition of axial velocity and streamline plot; $Co2.25pos3$, $C_T = 0.59$

from behind is generated vice versa to the one at the front face. An advantage of the turbine wake could be the deflection of the devices inner flow towards the diffuser wall and therein it contributes to the prevention of separation. Because the wake is oscillating and therefore this effect is unstable, an idea could be to place a solid structure behind the device to create an artificial but constant deflection in the wake area. Further investigations in this field are necessary, but not done within this study. If more energy is extracted, the flow through the Venturi device is decelerated more, while the flow around the structure is increasing in velocity, mass and deflection angle until the two wake areas close the structure from behind. The turbine at $pos3$ with the biggest disadvantage

concerning the blockage at the inlet operates with the highest thrust coefficient and withstands the highest pressure drop, respectively. But the highest power coefficients among the three positions is reached by the turbine at $pos1$. Fig. 20 show a storyboard for the flow development with the turbine implemented at position one.

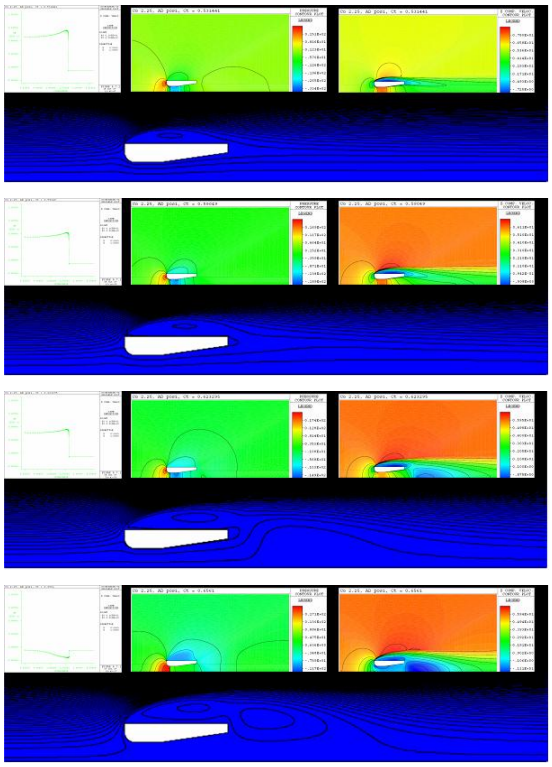

Figure 20: Streamline, AD velocity profile, pressure and axial velocity plots; $Co2.25pos1$, $C_T = 0.53$, $C_T = 0.59$, $C_T = 0.62$, $C_T = 0.66$

Co1.00AD: With the streamline plots for $Co1.00pos1$ (fig. 21) the growing separation bubble on the outer surface of the model is visible. Remarkable is the streamline tube widening behind the structure, resembling the expected streamline tube for a bare turbine. The typical streamline tube seems to be shortly interrupted by the structure and continues afterwards. The behaviour that can be observed is, the higher the deceleration of the wind velocity is the more narrows the 'supporting' streamline tube. For $C_T = 0.3$, for example, the inlet cross section of the streamline tube far in front of the structure is around $9m^2$ larger than for the case of $C_T = 0.53$. This also reflects the decreasing mass flow through the structure and actuator disc, respectively. However, the turbines position seems not to influence the performance in a significant way.

Comparison: The qualitative description of the

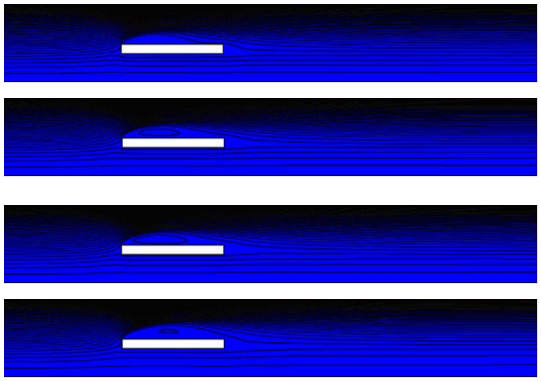

Figure 21: Streamline plots; $Co1.00AD$, $C_T = 0.30$, $C_T = 0.36$, $C_T = 0.44$, $C_T = 0.53$

untypical system $Co2.25AD$ flow behaviour and the explanation by the 'shield' at the front face and the 'blocking' at the rear face is not analytically defined. It could be the influence of the more or less deep located turbine with its pressure peaks. In contrast to the contraction of 2.25, the model with no Venturi shaping inside shows a very regular behaviour with no significant differences among the three turbine positions. Probably higher thrust coefficients would enforce more distinctive characters. For the $Co2.25AD$ model, $pos1$ turns out to be the most effective position, therefore its results are compared in the following with the $Co1.00pos1$ results. As mentioned earlier, to compare the two cases with the help of the power coefficient is difficult, because the rotor diameters are not the same, but the inlet diameter. In case of referring the power coefficient to the rotor area, the Betz maximum of $\frac{16}{27}$ is exceeded with $C_{P_4}(Co2.25pos1) = 0.69$ by 16.68%, while the thrust coefficient, referring to the rotor area as well, lies with $C_{T_4}(Co2.25pos1) = 0.53$ far below $\frac{8}{9}$. Which value can be directly used for comparison is the power itself.

$$P = C_P \frac{1}{2} \rho v_w^3 A_{rotor}. \tag{15}$$

The derived values are listed in tab. 3. An ideal bare turbine and its operation, one rotor with inlet diameter, big bare, and one rotor with throat diameter, small bare, is analytically calculated [13] and inserted in the same table. Although the $Co1.00AD$ model is not run for higher thrust coefficients, higher power values could be achieved certainly. But comparing the power maximum for the contraction 2.25, turbine positioned at $pos1$, with the power value achieved by the model without constriction but same pressure drop, shows the potential of the shaping combined with the right turbine positioning. To compare the turbine

	C_{T_1}	C_{T_2}	C_{T_3}	C_{T_4}
Co1.00				
$C_P\ [-]$	0.23	0.25	0.30	**0.31**
$power\ [W]$	1953	2115	2486	**2592**
Co2.25				
$C_P\ [-]$	**0.40**	0.47	0.55	0.69
$C_P^*\ [-]$	0.18	0.21	0.25	**0.31**
$power\ [W]$	**1506**	1756	2067	2586
big bare				
$C_P\ [-]$	0.28	0.33	0.38	0.45
$power\ [W]$	2319	2747	3233	3767
small bare				
$C_P\ [-]$	0.28	0.33	0.38	0.45
$power\ [W]$	1031	1221	1437	**1674**

Table 3: Flow characteristics overview, models without turbine

encased by the constricted tubing with the one encased by a constant diameter tubing the C_P^* seems to be a convenient coefficient, while the fact of the power harvesting by a smaller turbine is not reflected with it. Comparing the big bare rotor power with the power gained by the $Co1.00$ encased turbine, it performs better. Of course, it has to be remarked, that effects like tip loss reduction, varying thrust distribution etc. are not considered here and might change the conclusion. Definitely the comparison between a small bare rotor and the $Co2.25$ encased rotor is significant. The power amplification is 54.24%.

5 Conclusion

Within a comparison with bare turbines, the encased turbine, nine meters in diameter, produced less power than the bare turbine the same size. Reviewing the bare $Co1.00$ structure, already blocking the wind, a mean velocity of $5.35m/s$ was found in the device, which lies below the $6m/s$ for the approaching wind velocity. In contrast to that the $6m$ in diameter turbine, placed inside the Venturi shaped duct, seemed to be able to produce 54.24% more power than a bare turbine the same size. Regards to the different tip loss situations might lead to another result, but were not considered in this work. It also has to be mentioned, that this comparison is only valid for a constant wind direction. Thus comes a Venturi shaped casing compared to a straight duct with the advantages of a smaller rotor and with it lower production, transportation etc. costs and especially installation on high buildings with corresponding erection equipment might be more feasible or less complicated. Also important is due to the contracting inlet, the lowered turbulence intensity in the flow approaching the turbine. Furthermore is the Venturi effect amplifying the wind velocity and so the air velocity in the throat might be sufficient high to operate the turbine, while the big rotor experiencing velocities even below wind velocity still stands still. On the other hand is it very important to consider the changed loads situation on the building structure, which might needs to be strengthened, planned stiffer or may more flexible at certain locations. In general is an encasing for turbines in urban areas recommendable, e.g. in case of a blade loss the centrifugal energy will be first caught by the casing. Also frequently moving shadows, cast on buildings, could be reduced, due to the more hidden turbine. Lower adequate noise levels, demanded in towns, could be fulfilled by the possibility to integrate damping material in the encasing structure and probably directing of the sound waves. But these are already some topics which have to be investigated in further studies. It is not possible to integrate the Venturi shape without changing the appearance dramatically (fig. 22).

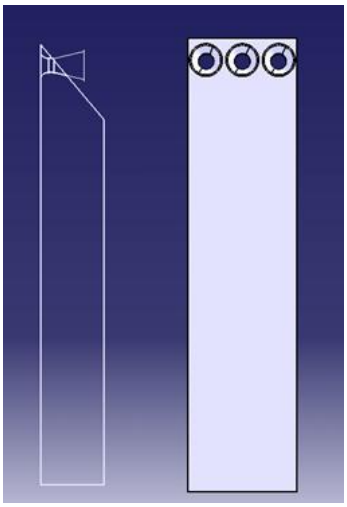

Figure 22: Venturi shape integrated in 'Castle House'

6 Future work

It was a challenge to restrict the parameter study and find constant parameter, respectively. Therefore a wide field for further investigations already exists only for the parameter study itself. So it would be interesting to know more about the flow behaviour with different wind velocities, influence of skewed inflow, regards to the tip loss situation, structure to prevent human hazard in case of

blade loss, considering of turbine fixing and nacelle structure and many more. The next step could be to go from the decoupled coin model back to the Venturi integrated in a building and take the whole structure geometry exposed to a wind velocity profile in urban areas into account. Probably a vertical skewed device build in angle could catch the upwind better to prevent separation in the inlet.

7 Acknowledgments

This work is dedicated to my beloved family.

References

[1] www.enflo-windtec.ch; 21^{st}March2008

[2] www.pacwind.net; 21^{st}March2008

[3] www.loopwing.co.jp; 21^{st}March2008

[4] www.aeroliftpatent.com; 21^{st}March 2008

[5] www.hushenergy.com; 21^{st}March 2008

[6] www.avinc.com; 21^{st}March 2008

[7] www.aerotecture.com; 21^{st}March 2008

[8] www.intelligenttravel.typepad.com; 21^{st}March 2008

[9] Van Bussel G. *The science of making more torque from wind: Diffuser experiments and theory revisited*; Conference Series 75. Journal of Physics, 2007

[10] Kühn M. *Windenergienutzung I*; lecture notes; Universität Stuttgart, 2006

[11] *DIN EN ISO 5167-3:2003*; Durchflussmessung von Fluiden mit Drosselgeräten in voll durchströmten Leitungen mit Kreisquerschnitt- Teil3: Düsen und Venturidüsen; DIN Deutsches Institut für Normung e. V. Berlin, Deutschland, 2003

[12] Barlow JB, Rae WHJr, Pope A. *Low-Speed Wind Tunnel Testing*; John Wiley & Sons, Inc., third edition, 1999

[13] Hansen MOL. *Aerodynamics of Wind Turbines*; James & James (Science Publishers) Ltd., London 2001